Synthesis and Biological Evaluation of New Pentaphyrin Macrocycles for Photodynamic Therapy

Clara Comuzzi,[†,#] Susanna Cogoi,[‡,#] Mark Overhand,[§] Gijs A. Van der Marel,[§] Herman S. Overkleeft,[§] and Luigi E. Xodo*[,‡]

Department of Chemical Science and Technology, University of Udine, Via del Cotonificio 108, 33100 Udine, Italy, Department of Biomedical Science and Technology, University of Udine, School of Medicine, Piazzale Kolbe 4, 33100 Udine, Italy, and Leiden Institute of Chemistry, Gorlaeus Laboratories, Leiden University, P.O. Box 9502, 2300 RA Leiden, The Netherlands

Received August 19, 2005

This paper describes the synthesis and in-depth characterization of two new porphyrogenic macrocycles **1** and **2**, and provides an evaluation of these molecules as photosensitizer agents. By tuning the reaction conditions and starting from readily available 1,9-diformyl-5-phenyldipyrromethane (**4**) and tripyrrane dicarboxylic acid (**3**), both the nonaromatic isopentaphyrin **1**, composed of a 24 π-electron macrocycle, and the aromatic pentaphyrin **2**, composed of a 22 π-electron macrocycle, were obtained in good yield and purity. Confocal laser microscopy and cytofluorimetry studies showed that the newly synthesized pentaphyrins penetrate the cell membranes and localize mainly in the cytoplasm. In the absence of light, **1** and **2** exhibit a nonsignificant cytotoxic effect at concentrations up to 3 μg/mL. In contrast, the synthesized pentaphyrins, when delivered to cells at 1.5 or 3 μg/mL and irradiated with white light (8 mW/cm^2), promoted a strong and dose-dependent phototoxic effect in four different cell lines. FACS and caspase-3/7 activation assays demonstrated that the pentaphyrins cause cell death by apoptosis.

Introduction

Photodynamic therapy (PDT) is a local treatment designed to eliminate abnormal tissue lesions, including cancer.[1−3] PDT involves the administration to the tumor tissue of a photosensitizer agent, which is subsequently activated by light. The activated photosensitizer transfers energy to molecular oxygen to generate reactive oxygen species (ROS), in particular singlet oxygen, with cell death as a result.[4−6] As reactions involving singlet oxygen occur in the immediate environment of the photosensitizer, the photodamage is confined to the tissue area that has been treated with light.[7]

A number of photosensitizers have been proposed for PDT;[8,9] however, the photosensitive compound most widely used in the clinic is Photofrin: a mixture of monomers, dimers, and oligomers derived from chemical manipulation of hematoporphyrins.[10] Although this preparation has proved to be efficacious for different types of cancer,[4] there are some limitations to its clinical use. Photofrin consists of about 60 compounds,[1] and its composition therefore is difficult to reproduce. Its longest absorption wavelength is 630 nm,[11,12] so the drug cannot be activated at longer wavelengths, which are more transparent to tissue. Like most porphyrinoid molecules, Photofrin also is absorbed by the skin, but it causes a longstanding cutaneous photosensitivity.[13] As PDT has the potential to become a major treatment in cancer photochemotherapy, efforts are being made to produce a new generation of photosensitizers with enhanced biological properties. In this context, we embarked on a program aimed at the preparation of expanded porphyrins, since previous studies have shown that these compounds have promising photosensitizing features.[14−16]

Several expanded porphyrins have been previously described, and recent findings show that some of these macrocycles may exist in different oxidation states,[17,18] with or without an aromatic π system. However, little is known about the biological properties of this class of compounds. In this paper, we describe the synthesis of two new macrocycles belonging to the class of pentaphyrins [1.1.1.1.1], namely, the nonaromatic macrocycle isopentaphyrin **1** (with 24 π-electrons) and the corresponding aromatic macrocycle **2** with 22 π-electrons, called pentaphyrin[19−22] (Figure 1). We also report a biological evaluation, performed on four different cell lines, of the two synthesized pentaphyrins. The cellular uptake of the pentaphyrins was analyzed by flow cytometry and confocal laser microscopy on live HeLa cells, while the cytotoxicity in the dark and after light treatment was evaluated by MTT and/or fluorimetric assays, under a variety of experimental conditions. Cell cycle analysis by flow cytometry and caspase 3/7 assays indicates that the synthesized pentaphyrins induce, following photoactivation, cell death by apoptosis.

Results and Discussion

Synthesis and Characterization of the Pentaphyrins. The synthesis of isopentaphyrin **1** was accomplished as shown in Figure 1. Treatment of known tripyrrane dicarboxylic acid **3**[23−25] with neat trifluoroacetic acid (TFA, 10 equiv) induces a double decarboxylation to obtain a reactive intermediate that is condensed with 1,9-diformyl-5-phenyldipyrromethane **4**.[26−29] Care needs to be taken that the final acid concentration is not too high to prevent degradation products. The reaction mixture was subsequently neutralized with triethylamine (TEA) under exclusion of light after which 2,3-dichloro-5,6-dicyano-1,4-benzoquinone (DDQ) was added. The best results, in terms of yield and purity of **1**, were obtained when using 2 equiv of DDQ as the oxidizing agent. Isopentaphyrin **1** was obtained after workup and HPLC purification as a green metallic film in 40% yield. The new compound **1** was characterized by a combination of HRMS spectrometry, NMR (COSY and NOESY) and UV−Vis spectroscopy. The ^{1}H NMR spectrum of isopentaphyrin

* To whom correspondence should be addressed. Tel (+39)0432.494395; fax: (+39)0432.494301; e-mail: lxodo@makek.dstb.uniud.it.
† Department of Chemical Science and Technology, University of Udine.
‡ Department of Biomedical Science and Technology, University of Udine.
§ Leiden University.
# These authors have equally contributed to this work.

10.1021/jm050831l CCC: $33.50
Published on Web 11/24/2005

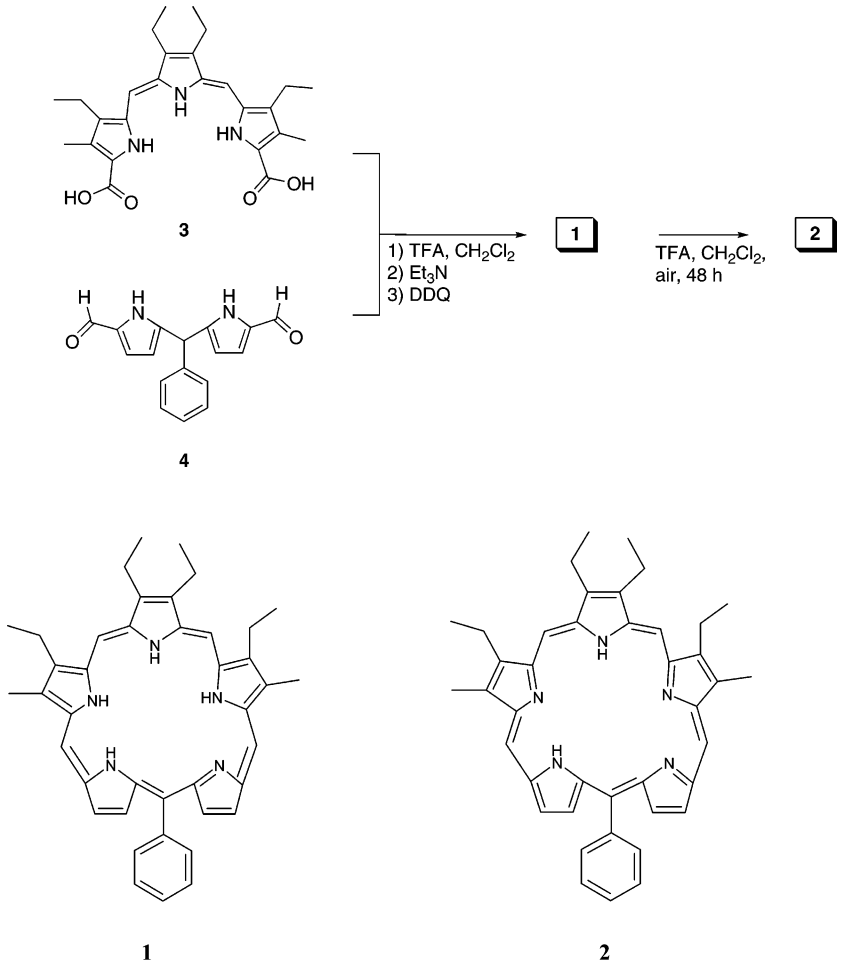

Figure 1. (Top) Synthetic route to isopentaphyrin **1** and pentaphyrin **2**; (bottom) molecular structures of isopentaphyrin **1** (20-Phenyl-2,13-dimethyl-3,7,8,12-tetraethyl-[24]isopentaphyrin) and pentaphyrin **2** (20-Phenyl-2,13-dimethyl-3,7,8,12-tetraethyl-[22]pentaphyrin). Isopentaphyrin **1** is characterized by a 24 π-electron nonaromatic macrocycle, while pentaphyrin **2** is characterized by a 22 π-electron aromatic macrocycle.

clearly demonstrated its nonaromatic character. The absence of a large ring current is indicated by the lack of the characteristic upfield shifts of NH protons which resonate at 12 and 11.6 ppm and of the downfield shifts of the *meso*-CH protons which are detected at 7.35 and 7.51 ppm (see Experimental Section and Supporting Information). The mass spectrum [HRMS *m*/*z* 606.35968 (MH^+), calculated for $C_{41}H_{44}N_5$ 606.35912] is consistent with structure **1** and shows that isopentaphyrin is not able to form adducts with small molecules such as water and methanol. The UV−Vis spectrum recorded in CH_2Cl_2 1% TFA shows a Soret-like band at 481 nm ($\log \epsilon = 4.2$) and a Q-band at 815 nm ($\log \epsilon = 3$).

As the next research objective, the oxidation of **1** to pentaphyrin **2** was investigated. In the first instance, treatment of **1** as the free base in chloroform with either DDQ or *p*-chloranil as the oxidizing agent were unsuccessful. However, at high acidity [>20% TFA (v/v) in $CHCl_3$] compound **1** was quantitatively oxidized to give **2** with DDQ, *p*-chloranil or air as the oxidant. Using the air oxidation has the advantage that after removal of the solvent no further workup or purification steps are required. The transformation of the nonaromatic isopentapyrin **1** into the aromatic pentaphyrin **2** was readily established by extensive (COSY, NOESY, HSQC) NMR experiments (see Supporting Information). It is worth noting that all the signals in compound **2** undergo a shift compared to **1** as a consequence of the ring current effect. For instance, the NHs experience a huge upfield shift: from 12 and 11.6 ppm in **1** to −1.82, −3.3, and −3.4 ppm in **2** (Experimental Section and Supporting Information). In contrast with its reduced species, the mass spectrometric studies revealed that pentaphyrin **2** is able to form complexes with small neutral molecules such as water and methanol. Adduct peaks can be detected in the mass spectrum: HRMS *m*/*z* 604.34418 (MH^+), calculated for $C_{41}H_{42}N_5$ 604.34347; $MH^+ - H_2O$ 622.35474 (622.35404); $MH^+ - CH_3OH$ 636.37048 (636.36969). A similar behavior was also observed with a tetrahydroxypentaphyirin derivative.[30] The UV−Vis spectrum recorded in CH_2Cl_2 10% TFA shows a Soret-like band at 473 nm ($\log \epsilon = 5$) and a Q-band at 655 nm ($\log \epsilon = 4$). Both compounds **1** and **2** proved to be stable in the solid state as well as in solution for prolonged time as detected by LC-MS, NMR and UV−Vis spectroscopies.

Pentaphyrin Uptake. The efficiency of a photosensitizer to induce photokilling depends on its capacity to penetrate the plasma membrane and accumulate in the target cell. To study the cellular uptake, we first asked if pentaphyrins **1** and **2** are stable in the presence of human serum. In DMSO, **1** and **2** show UV−Vis spectra with a typical high-intensity Soret band near 470 nm ($\log \epsilon \sim 3.8$ for **1**, $\log \epsilon \sim 4.9$ for **2**) and a low intensity broad band between 700 and 800 nm [$\log \epsilon \sim 3.1$ for **1** (770 nm), $\log \epsilon \sim 3.4$ for **2** (700 nm)] (Figure 2). In aqueous PBS containing 10% v/v bovine serum, the spectra showed a less intense Soret band, which is probably due to some degree of stacking of the macrocycles.[31] The observation that the absorption spectra did not change over a period of 24 h indicates that the synthesized pentaphyrins are stable in a serum-containing medium. The fluorescence emission spectra of pentaphyrins **1**

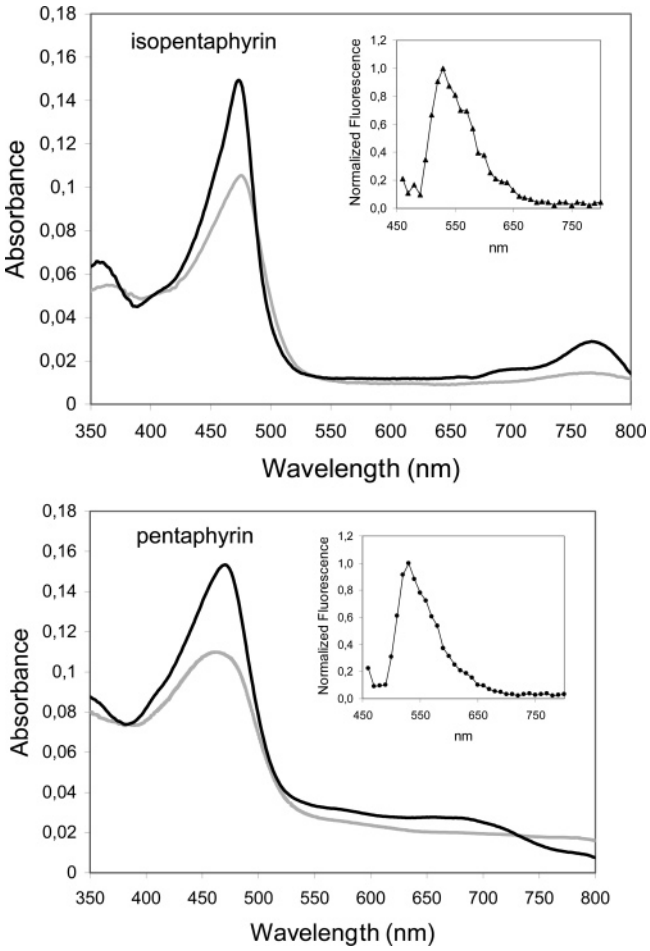

Figure 2. Absorption spectra of pentaphyrins **1** and **2** in DMSO (bold line) and PBS containing 10% (v/v) fetal bovine serum (gray line). Spectra have been recorded in a 0.5-cm path length cuvette, containing **1** (5×10^{-5} M) or **2** (2.5×10^{-5} M). Insets show normalized fluorescence spectra of pentaphyrin in the environment of lysed HeLa cells.

and **2** were measured in the environment of HeLa cells. Solutions containing 10 μM pentaphyrin and HeLa cells, which were lysed just before spectra acquisition, were excited at 420 nm, and emission spectra were recorded from 450 to 800 nm. The insets in Figure 2 report the fluorescence spectra and show that both pentaphyrins **1** and **2** emit fluorescence in the 500 to 600 nm range. Although the intensity of the fluorescence light was low, it was possible to investigate the capacity of the pentaphyrins to internalize in HeLa cells by flow cytometry and confocal laser microscopy. Figure 3 (top) shows the green fluorescence, measured by flow cytometry, that is associated with HeLa cells treated for 24 h with pentaphyrins **1** and **2** (3 μg/mL). The fluorescence associated with the cells treated with the aromatic pentaphyrin **2** showed a 3-fold increase, as a result of the drug uptake. By contrast, the increase of fluorescence observed with isopentaphyrin **1** was lower, suggesting that the reduced macrocycle has a lower capacity to enter the cells. Measuring the green fluorescence associated with HeLa cells as a function of time, we found that pentaphyrin **2** was taken up within 6−8 h, while isopentaphyrin **1** required a longer time (about 15 h). To study the cellular localization of the pentaphyrins, we performed confocal laser microscopy experiments with HeLa cells. In a first set of experiments, we analyzed the uptake in cells fixed on a glass slide and stained with propidium iodide, after permeabilization with Triton X-100. We observed that the pentaphyrins localized mainly in the cytoplasm (see Supporting Information). However, as it can be noted that the photosensitizer may relocate during the membrane permeabilization, we studied the localization of the pentaphyrins also in live HeLa cells, which were stained with hexidium iodide, a vital dye that binds to DNA and RNA and displays red fluorescence.[32] HeLa cells were treated with pentaphyrins and hexidium iodide, transferred to a Leica incubator, and analyzed on a confocal microscope under controlled temperature and CO_2. Figure 3 (bottom) shows projections of 10 cumulative xy-sections performed on untreated and pentaphyrin-treated cells. Panels A,D,G show the cells stained in red with hexidium iodide, panels B,E,H show the fluorescence green light emitted by the pentaphyrins, while panels C,F,I show the superimposition of A−B, D−E, and G−H images. It can be seen that the green light emitted by the pentaphyrins appears to be localized in the cytoplasm, indicating that the pentaphyrins do not accumulate in the nuclei. The fact that the new synthesized pentaphyrins do not localize in the nucleus suggests that their potential to cause DNA damage, mutations, and carcinogenesis is expected to be low.[33]

Cytotoxycity of the Pentaphyrins without Light Irradiation. The biological activity of pentaphyrins **1** and **2** was evaluated in four different human cell lines: (i) chronic myelogenous leukemia K562; (ii) transformed fibroblast IMR90 E1A; (iii) pancreatic adenocarcinomas Panc-1; and (iv) cervix adenocarcinomas HeLa. An important prerequisite that a photosensitizer should have is a low cytotoxicity when it is not irradiated. We therefore measured the cytotoxicity of **1** and **2** in the dark, by means of MTT assays. Compounds **1** and **2** were delivered to the cells without using any transfecting agent, and the percentage of viable cells was evaluated 24 and 48 h after treatment with increasing amounts of **1** or **2** (up to 12 μg/mL final concentration). Figure 4 shows the results obtained by treating the four cell lines with 1.5, 3, 6, 9, and 12 μg/mL pentaphyrins **1** and **2**. After 24 and 48 h of incubation in the dark, the percentage of viable cells in each sample was measured by MTT assays. At low pentaphyrin concentrations (<3 μg/mL), the cells were not particularly affected by the treatment with the pentaphyrins, whereas at concentrations >3 μg/mL, **1** and **2** exhibited a significant cytotoxic effect in K562 and IMR90 E1A cells. By contrast, in Panc-1 and HeLa cells the toxic effect induced by **1** and **2** was very low even at high drug concentrations. The IC_{50} evaluated 24 h after pentaphyrin treatment varied from 16 to 42 μg/mL. They are more than 1 order of magnitude higher than the IC_{50} (0.9 μg/mL) reported for a pentapyrrolic macrocycle previously tested in Jurkat E6-1 cells.[30]

Phototoxycity Induced by the Pentaphyrins in Cultured Cells. We measured the phototoxicity of pentaphyrins **1** and **2** in the concentration range 0.6−3 μg/mL, i.e., under conditions in which the compounds did not show an appreciable cytotoxic effect in the tested cell lines. The cells were treated with **1** or **2** (previously dissolved in DMSO) for 24 h, then irradiated with a metal halogen white lamp at an irradiance of 8 mW/cm^2. Cell proliferation was measured by the CellTiter-Blue Cell Viability assay, a fluorimetric method for the estimation of the viable cells in multiwell plates. As a control, we used untreated and DMSO-treated cells irradiated for the same amount of time and with the same light intensity used for the PDT experiments. Figure 5 shows the percentage of viable cells incubated for 24 h with **1** or **2** at concentrations of 0.6, 1.5, and 3 μg/mL and irradiated with white light (irradiance: 8 mW/cm^2) for 30 or 60 min. Left panels show the percentage of cell viability immediately after irradiation. It can be seen that the immediate

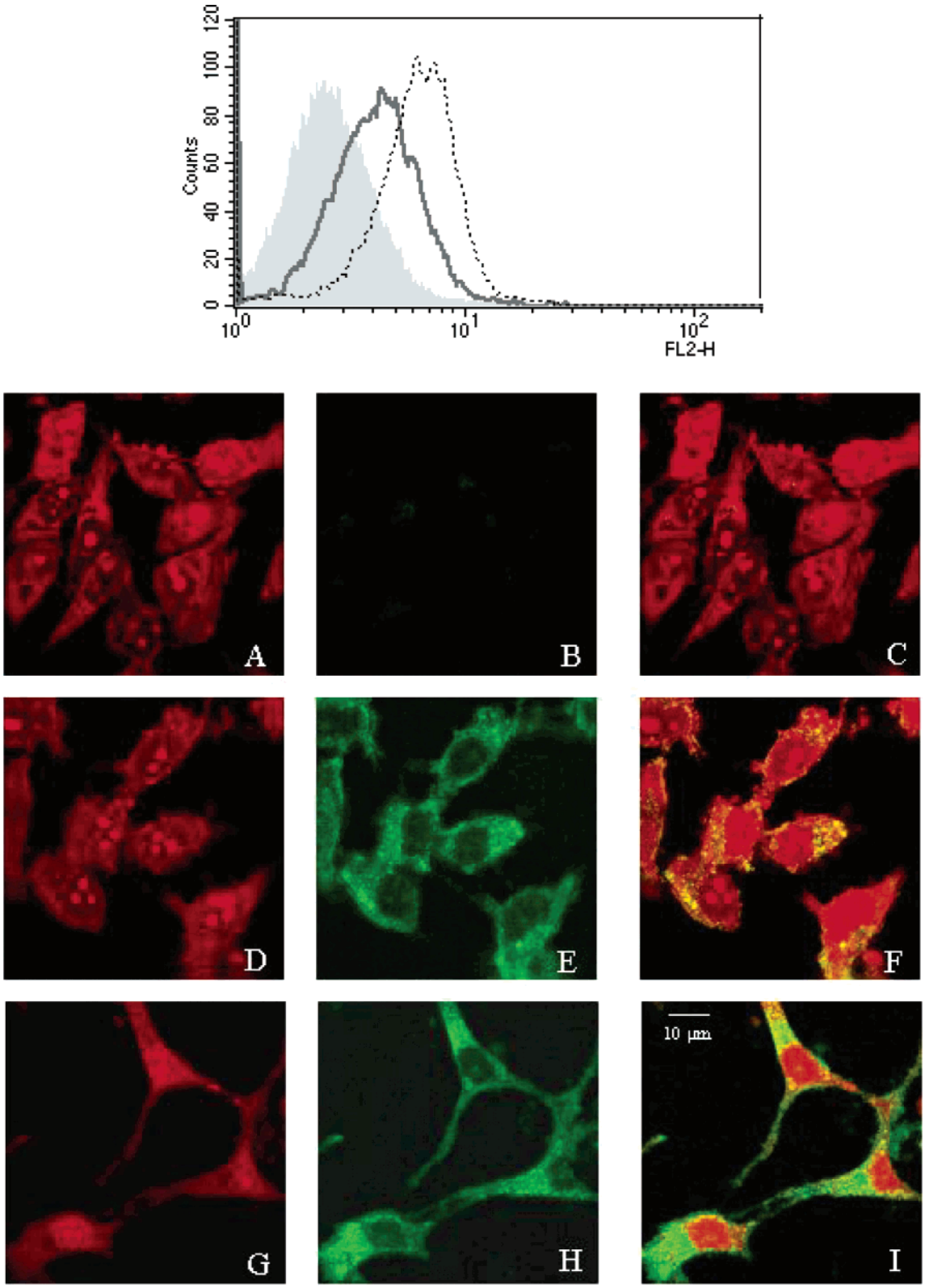

Figure 3. (Top) FACS analysis of untreated (filled peak), 3 μg/mL isopentaphyrin **1**-treated (bold-line peak) and 3 μg/mL pentaphyrin **2** -treated (dashed-line peak) HeLa cells. The photosensitizers were delivered to the cells without any transfecting agent. The filled peak represents the basal fluorescence associated with the drug-untreated cells, whereas the bold- and dashed-line peaks represent the acquired fluorescence due to the uptake of isopentaphyrin **1** and pentaphyrin **2**, respectively; (bottom) confocal laser micrographs of live HeLa treated for 24 h with 3 μg/mL pentaphyrins **1** (panels D−F) and **2** (panels G−I). Untreated cells (panels A−C). Panels A, D, and G show live HeLa cells stained with the vital dye hexidium iodide; panels E and H show the green fluorescence emitted by the pentaphyrins internalized in the cytoplasm; panels C, F, and I are the superimposition of panels A−B, D−E, and G−H.

effect of the light treatment, which should account for early necrotic death, is barely detectable. Therefore, we reincubated the cells for a further 24 h before proceeding with the cell viability assay (right panels). In this case, we observed a dramatic reduction of cell viability, which is proportional to the irradiation time and to the amount of pentaphyrin delivered.

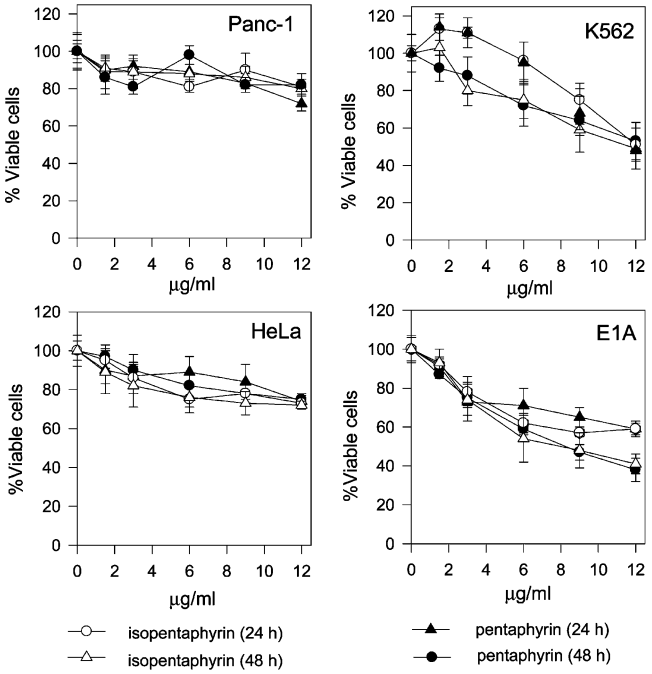

Figure 4. Cytotoxicity of pentaphyrins **1** and **2** in the absence of light on four different cell lines. Ordinate reports the percentage of viable cells as a function of pentaphyrin concentration. Cells were incubated with the pentaphyrins either for 24 or 48 h in the dark, MTT assays were then performed. The data shown are the means ±SD of three independent experiments done in triplicate.

The delayed post-irradiation death is likely due to secondary necrosis and apoptosis induced by pentaphyrin-mediated photodynamic effects. The experiments were repeated by reducing to 4 h the preincubation of the cells with the pentaphyrins before irradiation. In this case, a weaker PDT effect was obtained, in particular with isopentaphyrin **1**, likely due to a lower amount of pentaphyrin taken up by the cells. We estimated the IC_{50} for the pentaphyrins and reported the data in Table 1. The following observations can be made: (a) the photodynamic effect depends on irradiation time. For instance, IC_{50} values of the aromatic pentaphyrin **2** measured in cells irradiated for 30 min are 20 to 60% higher that the values obtained with an irradiation time of 60 min; (b) The nonaromatic isopentaphyrin **1** appears to be a less efficient photosensitizer than the aromatic pentaphyrin **2**, at all conditions used (15 or 30 J/cm^2, 4 or 24 h preincubation); (c) Panc-1 cells are most resistant to the photokilling by the aromatic pentaphyrin **2**; this is in line with the observation that pancreatic adenocarcinomas cells are particularly resistant to any form of chemotherapy treatment.[34]

The phototoxicity of pentaphyrins **1** and **2** on leukemic K562 cells can be directly compared with that observed with Photofrin and thioglycosylated porphyrins derivatives.[35] In a previous study, K562 cells were treated with 1.2 μg/mL Photofrin and porphyrin derivatives and irradiated for different times (up to 120 min) with white light at 5 mW/cm^2. The dead cells were counted immediately after irradiation and after a 24 h incubation in the dark, i.e., under experimental conditions very similar to those used in our study. The results obtained with an irradiation of 60 min show that both Photofrin and thioglycosylated porphyrins induced a 24 h post-irradiation death similar to that promoted by the aromatic pentaphyrin **2** (60−80% dead cells). By contrast, the immediate irradiation effect, which probably accounts for early necrotic death, was significant for Photofrin (20% cell death) and thioglycosilated porphyrins (80% cell death), but it was under the detectable level for the aromatic pentaphyrin **2**. This suggests that pentaphyrin **2** activates a photokilling effect that is likely due to apoptosis rather than necrosis.

PDT-Induced Apoptosis. The discovery that PDT can trigger apoptosis in cancer cells has provided a molecular rationale for the photokilling observed in the treated cells.[36] As the new synthesized pentaphyrins produced a strong photodynamic effect in four different cell lines tested, we addressed the question whether cell death was due to apoptosis. Apoptosis is a natural mechanism leading to cell death resulting in the cleavage of nuclear DNA and fragmentation of the cells into small particles. Generally, malignant cells have a lower capacity to activate apoptosis than normal cells: an effect that confers resistance to chemotherapy.[37,38] We therefore analyzed by FACS, through the staining of the cellular DNA content with propidium iodide, whether the treatment of K562 and IMR90 E1A cells with 3 μg/mL **1** or **2** and irradiation for 60 min, at 8 mW/cm^2 induced the typical apoptotic fragmentation of the cells and nuclei. The result of this experiment is shown in Figure 6. It can be seen that following light treatment the cell cycle changes, with the appearance of the typical pre-G1 apoptotic broad peak,[39] due to the cell apoptotic bodies caused by the photodamage. It is worth noting that the cells treated with the aromatic pentaphyrin **2** showed a stronger pre-G1 peak than the cells treated with pentaphyrin **1**, which is in keeping with the proliferation assays. To gain further insight into the nature of the photokilling induced by the pentaphyrins, we measured the activation of the caspase-3/7 in IMR90 E1A and K562 cells. Caspases are cystein proteases activated during the execution phase of apoptosis that play a key effector role in apoptosis in mammalian cells.[40−42] Their levels in untreated and pentaphyrin-treated K562 and IMR90 E1A cells were measured by the Apo-ONE caspase-3/7 assay. In accord with the FACS results, the activity of the caspases-3 and -7 strongly augmented in the cells treated with pentaphyrins and light. Also in this case pentaphyrin **2** is found to activate the caspases more efficiently than the reduced analogue **1**. Thus, FACS and caspase-activity data clearly suggest that the cell death produced by the synthesized pentaphyrins is due to apoptosis.

Conclusion. In this paper, we described the synthesis and characterization of two new pentaphyrin macrocycles showing a strong PDT effect on different cancer cell lines. The two expanded pentaphyrins are characterized by a different oxidation state. The 24 π-electron macrocycle, named isopentaphyrine (**1**), was obtained by treatment of tripyrrane dicarboxylic acid (**3**) with trifluoroacetic acid, and this provided an intermediate that was condensed with 1,9-diformyl-5-phenyldipyrromethane (**4**). Isopentaphyrin **1** provided by oxidation with air or DDQ a 22 π-electron macrocycle that is, according to NMR spectra, aromatic in nature. UV−visible spectra show that the new synthesized pentaphyrins absorb between 700 and 800 nm allowing the use of wavelengths at which light is slightly absorbed by heme proteins and other compounds in the tissues. In a cellular environment, the pentaphyrins exhibit a fluorescence emission in the 500−600 nm range. The biological properties of the two expanded pentaphyrins were investigated by a variety of techniques. Cytofluorimetry and confocal laser microscopy showed that the pentaphyrins are capable of penetrating the cell membrane. Confocal laser microscopy, performed either on glass-fixed cells or directly on live cells, clearly demonstrates that the pentaphyrins localize in the cytoplasm. In the dark, the pentaphyrins were found to be nontoxic at concentrations ≤ 3 μg/mL and when irradiated with

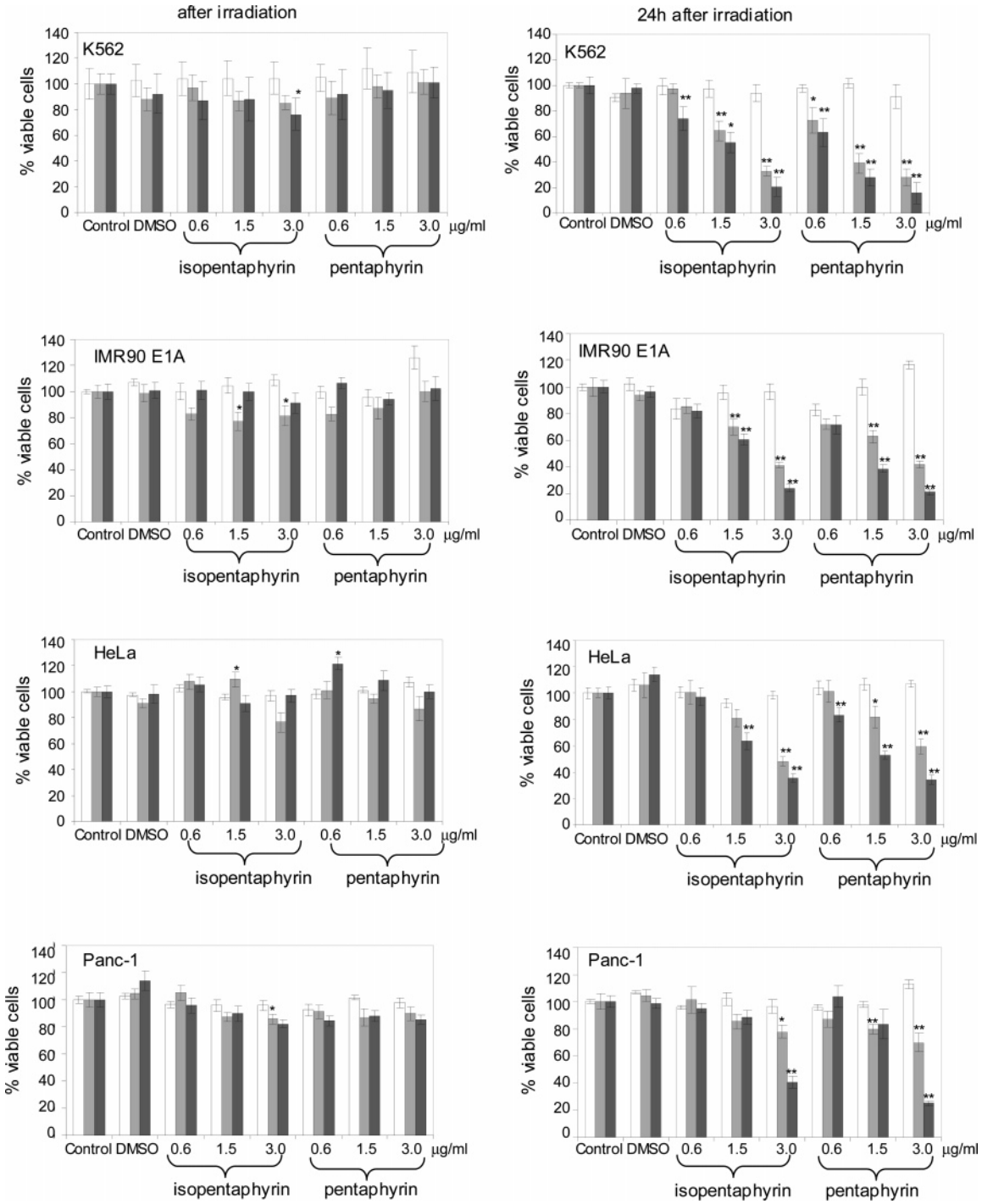

Figure 5. Phototoxicity of pentaphyrins **1** and **2** on four different cell lines. Cells were treated with the pentaphyrins at three different concentrations (0.6, 1.5, 3 μg/mL) and irradiated with white light (fluence rate: 8 mW/cm^2) for 30 or 60 min. Viable cells were measured by the CellTiter-Blue Cell Viability Assay (Promega). The histograms report in ordinate the percent of viable cells, i.e., the ratio $(RFU_T)/(RFU_C) \times 100$, where RFU_T is the fluorescence of treated cells, while RFU_C is the fluorescence of untreated cells. The histograms in the left panels show the cell photokilling immediately after irradiation, while those in the right panels show the photokilling 24 h after irradiation. Open bars: % viable cells of untreated cells; light gray bars: % viable cells after 30 min irradiation; dark gray bars: % viable cells after 60 min irradiation. The data shown are the means ± SE of three independent experiments done in triplicate. A standard *t*-test versus control was performed (**: $P < 0.01$; *: $P < 0.05$).

white light at fluencies of 15 or 30 J/cm^2, they promoted a strong photodynamic effect that caused cell death in all four cell lines analyzed. The aromatic pentaphyrin **2** appeared to be a more efficient photosensitizer than the nonaromatic analogues macrocycle **1**. The photodynamic effect promoted by pentaphyrins **1** and **2** caused cell death by apoptosis, as suggested by the appearance in the cell cycle profile of a typical pre-G1 peak and the activation of caspase-3 and caspase-7. Finally, literature data allowed the comparison of the synthesized pentaphyrins with Photofrin and some thioglycosylated porphyrins. The PDT effect induced by the photosensitizers on K562 cells was roughly comparable. By contrast, pentaphyrin **2** was found to trigger a cell-death mechanism mainly due to apoptosis, whereas Photofrin and thioglycosylated porphyrins were found to induce cell death by both apoptosis and necrosis. In conclusion, the results reported in this paper suggest that new synthesized pentaphyrins, in particular, the aromatic molecule **2**, may be effective therapeutic agents to be used in PDT.

Table 1. IC_{50} Values[a] (μg/mL) for Pentaphyrin (**2**) and Isopentaphyrin (**1**) Measured on Different Cell Lines Irradiated with White Light at the Fluence of 15 and 30 J/cm^2

	15 J/cm^2		30 J/cm^2	
	2	**1**	**2**	**1**
Panc-1	9.7	9.8	3.9	4.6
K562	2.0	3.6	1.5	2.9
HeLa	4.8	5.8	2.6	3.8
E1A	4.0	4.2	2.3	3.2

[a] Values have been obtained from plots reporting the % cell viability as a function of pentaphyrin/isopentaphyrin concentration. Uncertainty is ± 15%.

Experimental Section

Chemistry. All compounds were used as received from the suppliers. Analytical LC/MS was conducted on a JASCO system using an Alltima C_{18} analytical column (5μ particle size, flow: 1.0 mL/min). Absorbance was measured at 214 and 254 nm. Solvent System: A: 100% water, B: 100% acetonitrile, C: 0.5% TFA. Gradients of B were applied over 30 min unless stated otherwise. Mass spectra were recorded on a Perkin-Elmer Sciex API 165 equipped with a custom-made Electrospray Interface (ESI). Purifications were conducted on a BioCAD "Vision" automated HPLC system (PerSeptive Biosystems, inc.), supplied with a semipreparative Alltima C18 column (5μ particle size, running at 4 mL/min). Solvent system: A: 100% water, B: 100% acetonitrile, C: 1% TFA. Gradients of acetonitrile (B) in (A) containing 10% of C were applied over 3 column volumes (CV). ^{1}H NMR and ^{13}C NMR spectra were recorded on a Bruker 200 MHz, a Bruker AV-400 (400/100 MHz) or a Bruker DMX- 600 (600/150 MHz) spectrometer. Chemical shifts are given in ppm (δ) relative to tetramethylsilane (^{1}H NMR) as an internal standard or to the peak of the solvent used (^{13}C NMR). UV−Vis spectra were measured on a Jasco V-530 (Japan) spectrophotometer using either a 0.2 or a 0.5 cm quartz cuvettes, whereas fluorescence spectra were obtained with a Spectra MAX Gemini XS fluorometer (Molecular Devices Corp, Sunnyvale, Ca).

Isopentaphyrin 1. (20-Phenyl-2,13-dimethyl-3,7,8,12-tetraethyl-[24]isopentaphyrin) 100 mg (0.22 mmol) of **3**[23−25] was dissolved in 200 μL of TFA and stirred under Argon for 10 min at room temperature. The mixture was diluted with 20 mL of dry degassed dichloromethane. A solution of **4**[26−29] in dry degassed dichloromethane (62 mg, 0.2 mmol, in 5 mL) was immediately added with exclusion of light and stirred for 2 h. The solution was then cooled in an ice bath and neutralized dropwise with triethylamine. DDQ (91 mg, 0.4 mmol) was added, the ice bath was removed, and the solution stirred for 30 min. The solution was washed with water and evaporated to give a dark metallic green film. The residue was first chromatographed on N-Super I alumina with ethyl acetate to remove higher polymers and then purified by semipreparative HPLC (48 mg, 0.08 mmol, 40%). ^{1}H NMR 400 MHz ($CDCl_3$ 50% TFA) 12.03 (s 2H, NH), 11.6 (s 2H, NH), 7.85 (t, 2H, H phenyl), 7.6 (m, 2H, H phenyl), 7.51 (s, 2H, meso-CH), 7.49 (t, 1H, H phenyl), 7.35 (s, 2H, meso-CH), 7 (dd, 2H, H pyrrole), 6.74 (dd, 2H, H pyrrole), 2.8 (q, 4H, CH_2 ethyl), 2.7 (q, 4H, CH_2 ethyl), 2.2 (s, 6H, CH_3), 1.34 (t, 6H, CH_3 ethyl), 1.22 (t, 6H, CH_3 ethyl). HRMS 606.35968 (606.35912). UV−Vis (CH_2Cl_2 containing 1% TFA) shows a Soret-like band at 481 nm ($\log \epsilon = 4.2$) and a Q-band at 815 nm ($\log \epsilon = 3$).

Pentaphyrin 2. (20-Phenyl-2,13-dimethyl-3,7,8,12-tetraethyl-[22]pentaphyrin) 20 mg (0.033 mmol) of **1** was dissolved in 2 mL of $CHCl_3$/TFA 1/1. The dark solution was stirred for 2 days in the air at room temperature. The reaction mixture was washed with 10% NaOH solution and then washed with distilled water. The conversion of **1** to **2** was quantitative. ^{1}H NMR ($CDCl_3$ containing 10% TFA) 11.7 (s, 2H, meso-CH); 11.5 (s, 2H, meso-CH); 9.8 (d, 2H, H pyrrole); 9.2 (d, 2H, H pyrrole); 8.72 (m, 2H, H phenyl); 8.2 (m, 3H, H phenyl); 4.56−4.45 (2q overlapping, 8H, CH_2 ethyl); 4.07 (s, 6H, CH_3); 2.1−2 (2t overlapping, 12H, CH_3 ethyl); −1.82 (br s 1H, NH), −3.3 (br s 2H, NH), -3.4 (br s 2H, NH). HRMS 604.34418 (604.34347); $MH^+ \cdot H_2O$: 622.35474 (622.35404); $MH^+ \cdot CH_3OH$: 636.37048 (636.36969). UV−Vis (CH_2Cl_2 containing 10% TFA) 473 ($\log \epsilon = 5$); 655 ($\log \epsilon = 4$).

Cell Cultures. Human exocrine pancreas epithelioid adenocarcinoma cells (Panc-1), human lung E1A transformed fibroblast (IMR90 E1A), human epithelial cervix adenocarcinoma cells (HeLa) were cultured in DMEM medium; human chronic myelogenous leukemia cells (K562) were cultured in RPMI medium. Both media were supplemented with 100 U/mL penicillin, 100 μg/mL streptomycin, 200 mM L-glutamine, and 10% fetal bovine serum.

PDT and Evaluation of Cell Viability. Cytotoxicity experiments were performed with a 96-well microtiter plate in which each well contained in 100 μL of culture medium 5000 cells either untreated or treated with the pentaphyrins. After addition of pentaphyrin, the cells were dark-incubated for 24 h. The medium was substituted with PBS, and the cells were then irradiated either for 30 or 60 min with a white light from a Solaris 2 (J615) projector (150 W) at a fluence rate of 8 mW/cm^2. After irradiation, half of the cells was incubated for further 24 h in the dark in growth medium and then analyzed. The other half of the cells were immediately treated with the CellTiter-Blue mix (60 μL in each well) for measuring the cell viability. After 1 h incubation with the mix, the wells were analyzed with a Spectra MAX Gemini XS fluorometer (Molecular Devices Corp, Sunnyvale, Ca). The fluorometer wavelengths were set as follows: excitation 535 nm; cutoff 570 nm; emission 590 nm. Each experiment was conducted in triplicate. Data shown are the average of at least three independent experiments.

FACS Analysis. (Uptake) Uptake experiments studied by FACS were performed on HeLa cells. 8×10^4 HeLa cells were plated in DMEM medium and treated with 3 μg/mL pentaphyrins **1** and **2** for 24 h. After the treatment the cells were harvested, washed three times with PBS and analyzed by FACS; (apoptosis) (a) K562 cells (1.5×10^5) were treated with 3 μg/mL pentaphyrins **1** and **2** for 24 h in RPMI medium. The cells were then centrifuged, resuspended in PBS, and irradiated with light for 30 min (fluence at 8 mW/cm^2) or 60 min. After irradiation, the cells were incubated for 8 h in the dark in RPMI medium, harvested and then washed twice in PBS. The cells were then fixed overnight with 70% ethanol and stained for 1 h with propidium iodide (0.05 mg/mL) and RNase A (0.1 mg/mL). The cells were then analyzed by FACS (Becton Dickinson); (b) E1A cells (3×10^4) were plated in DMEM medium and treated as described in (a) but analyzed 16 h following irradiation.

Caspase Assay. We performed Caspase activity assays using Apo-ONE Homogeneous Caspase-3/7 assay (Promega), according to the manufacturer's protocol. 7.5×10^3 IMR90 E1A cells or 5×10^4 K562 cells were treated with 1.5 μg/mL pentaphyrins **1** and **2** for 24 h. The cells were irradiated in PBS for 30 min (fluence at 8 mW/cm^2) or 60 min. After irradiation, the cells were incubated for 16 h (E1A) or 8 h (K562) in the dark in growing medium. Then Homogeneous Caspase-3/7 reagent (substrate was dilute 1:100 with provided buffer) was added maintaining a 1:1 ratio of reagent to sample. The measure of fluorescence of each well was read at an excitation wavelength of 485 ± 20 nm and an emission wavelength of 530 ± 25 nm (Spectra Max Gemini XS, Molecular Devices Corporation, CA).

Confocal Microscopy and Spectroscopic Measurements. HeLa cells were seeded in glassed bottom Petri dishes at a density of 8×10^4 cells in 1 mL of DMEM medium supplemented with 10% fetal bovine serum. The cells in culture medium were incubated for 24 h with 6 μg/mL pentaphyrins **1** and **2**. Two hours before the end of the incubation 3 μM hexidium iodide was added to the cell medium. Hexidium iodide is a vital dye that binds to DNA and RNA and display red fluorescence upon excitation with a He−Ne laser light at 543 nm. Both the cytoplasm and the nucleus of HeLa cells treated with hexidium iodide are stained in red. Before the acquisition of the confocal images, the growing medium was replaced with a PBS solution and the Petri dish containing the cells was placed in a LEICA incubator that maintained a 5% CO_2 atmosphere and a temperature of 37 °C during the acquisition. The confocal images were obtained on a Leica DM IRBE confocal

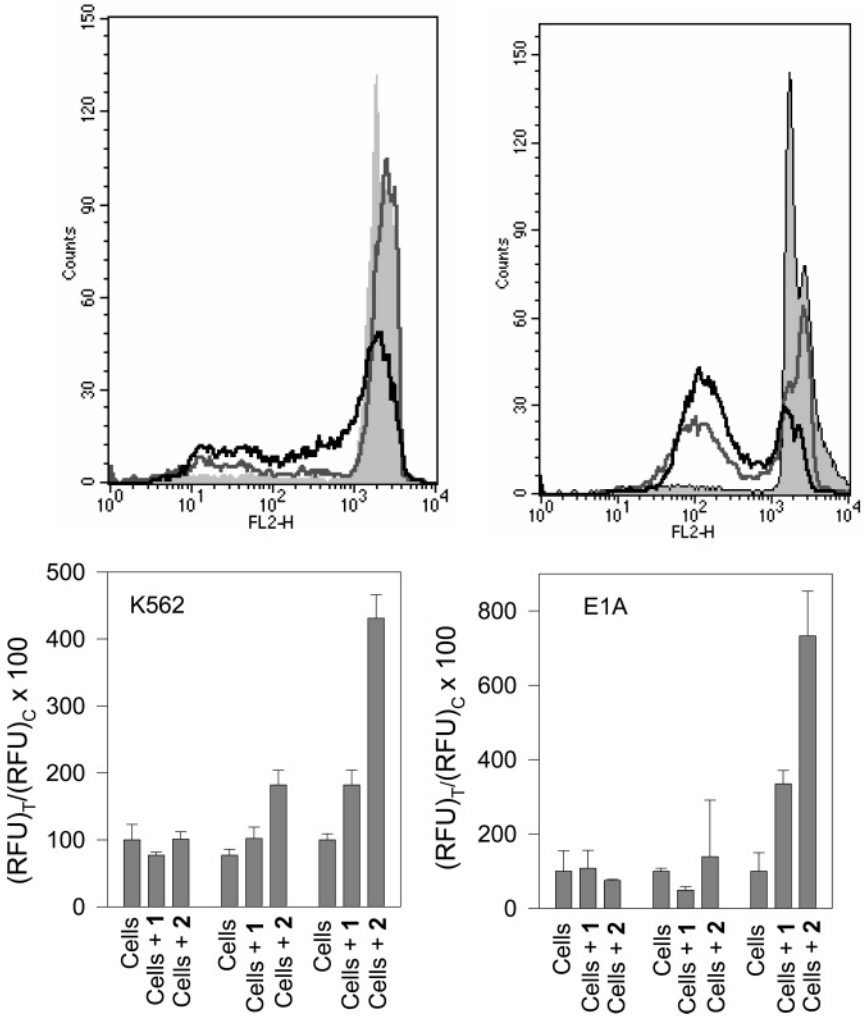

Figure 6. (Top) FACS analysis performed on K562 (left) and IMR90 E1A (right) cells untreated and treated for 24 h with 3 μg/mL pentaphyrins **1** and **2** and irradiated at 30 J/cm^2. Filled peak shows the cell cycle profile of untreated cells; gray-line peak shows the cell cycle profile of isopentaphyrin-treated cells; black-line peak shows the cell cycle profile of pentaphyrin-treated cells; (bottom) apoptosis assay showing the activity of caspases 3/7 in untreated or pentaphyrin-treated K562 and IMR90 E1A cells. Cells were incubated with 3 μg/mL of pentaphyrins **1** or **2** for 24 h; 8 h (K562) and 16 h (E1A) after irradiation for 15 or 30 J/cm^2, Apo-ONE caspase-3/7 assay was performed. The data shown are the means $\pm$ SD of three independent experiments. The histograms report in the ordinate the ratio $RFU_T/RFU_C \times 100$, where RFU_T is the fluorescence of treated cells and RFU_C the fluorescence of untreated cells. From left: bars 1−3 show the caspase assay performed on cells not irradiated; bars 4−6 show the caspase assay on cells irradiated for 30 min; bars 7−9 show the caspase assay on cells irradiated for 60 min. Irradiation was performed with white light at a fluence of 8 mW/cm^2.

imaging system, exciting the pentaphyrins with a 488 nm Argon laser light and detecting the green fluorescence emitted between 500 and 535 nm. Hexidium iodide was excited at 543 nm with a He−Ne laser light and the emission fluorescence was detected in the 640−680 nm interval.

Absorption spectra were recorded on a Perkin-Elmer UV−Vis spectrometer Lamba 14 using a 0.5-cm quartz cuvette, while emission spectra were recorded on a Spectra Max Gemini XS Microplate spectrofluorometer: excitation 420 nm and emission from 450 to 800 nm. To measure the fluorescence emission in the environment of HeLa cells, 10 μM pentaphyrins were incubated for 24 h with 6000 HeLa cells in 100 μL culture medium. Before spectra acquisition, the medium was replaced with PBS, and the cells were lysed. The spectra shown have been subtracted for the background fluorescence.

Acknowledgment. This study was supported by the Italian Ministry of University and Scientific Research (Prin 2003) and Area Science Park Trieste (Italy) (Progetto D4, Intervento B4). We thank Prof. C. Brancolini for providing IMR90 E1A cells.

Supporting Information Available: (a) ^{1}H spectra, chemical shifts values, NOESY, and COSY correlations for pentaphyrins **1** and **2**; (b) confocal laser microscopy images of glass-fixed HeLa cells treated with pentaphyrins **1** and **2** and propidium iodide. This material is available free of charge via the Internet at http://pubs.acs.org.

References

(1) Dolmans, D. E.; Fukumura, D.; Jain, R. K. Photodynamic therapy for cancer. *Nat. Rev. Cancer* **2003**, *3*, 380−387.
(2) Sibata, C. H.; Colussi, V. C.; Oleinick, N. L.; Kinsella, T. J. Photodynamic therapy in oncology. *Expert. Opin. Pharmacother.* **2001**, *2*, 917−927.
(3) Dougherty, T. J. An update on photodynamic therapy applications. *J. Clin. Laser Med. Surg.* **2002**, *20*, 3−7.
(4) Dougherty, T. J.; Gomer, C. J.; Henderson, B. W.; Jori, G.; Kessel, D.; Korbelik, M.; Moan, J.; Peng, Q. Photodynamic therapy. *J. Natl. Cancer Inst.* **1998**, *90*, 889−905.
(5) Miller, J. Photodynamic Therapy: the sensitization of cancer cells to light. *Chem. Educ. Today* **1999**, *76*, 592−594.
(6) Pervaiz, S. Reactive oxygen-dependent production of novel photochemotherapeutic agents. *FASEB J.* **2001**, *15*, 612−617.
(7) Moan, J.; Berg, K. The photodegradation of porphyrins in cells can be used to estimate the lifetime of singlet oxygen. *Photochem. Photobiol.* **1991**, *53*, 549−53.
(8) Allison, R. R.; Downie, G. H.; Cuenca, R.; Hu, X.-H.; Childs, C. J. H.; Sibata, C. H. Photosensitizers in clinical PDT. *Photodiagn. Photodyn. Ther.* **2004**, *1*, 27−42.

(9) Bonnett, R.; Berembaum, M. C. HpD-a study of its components and their properties. *Adv. Exp. Med. Biol.* **1983**, *160*, 241−250.
(10) Dogherty, T. J. A brief story of clinical photodynamic therapy development at Roswell Park Cancer Institute. *J. Clin. Laser Med.* **1996**, *14*, 219−221.
(11) Stenberg, E. D.; Dolphin, D.; Bruckner, C. Porphyrin-based photosensitizers for use in photodynamic therapy. *Tetrahedron* **1998**, *54*, 4191−4202.
(12) Dolphin, D. Photomedicine and Photodynamic Therapy. *Can. J. Chem.* **1994**, *72*, 1005−1013.
(13) Sibata, C. H.; Colussi, V. C.; Oleinick, N. L.; Kinsella, T. J. Photodynamic therapy in oncology. *Exp. Opin. Pharmacother.* **2001**, *2*, 917−927.
(14) Sessler, J. L.; Seidel, D. Synthetic Expanded Porphyrin Chemistry. *Angew. Chem. Int. Ed.* **2003**, *42*, 5134−5175.
(15) Jasat, A.; Dolphin, D. Expanded Porphyrins and Their Heterologs. *Chem. Rev.* **1997**, *97*, 2267−2340.
(16) Lang, K.; Monsinger, J.; Wagnerova, D. M. Photophysical properties of porphyrinoid sensitizers non-covalently bound to host molecules; models for photodynamic therapy. *Coord. Chem. Rev.* **2004**, *248*, 321−350.
(17) Shin, Ji.-Y.; Furuta, H.; Osuka, A. N-Fused Pentaphyrin. *Angew. Chem., Int. Ed.* **2001**, *40*, 619−621.
(18) Srinivasan, A.; Ishizuka, T.; Furuta, H. Doubly N-fused Pentaphyrins. *Angew. Chem., Int. Ed.* **2004**, *43*, 876−879.
(19) Khoury, R. G.; Jaquinod, L.; Nguyen, L. T.; Smith, K. M. Macrocycles containing five pyrrole subunits: the Iso-oxopentaphyrin System. *Heterocycles* **1998**, *47*, 113−119.
(20) Danso-Danquah, R. E.; Xie, L. Y.; Dolphin, D. Characterization of Decamethyl and Ethoxycarbonyl Pentaphyrins. *Heterocycles* **1995**, *41*, 2553−2564.
(21) Krivokapic, A.; Cowley, A. R.; Anderson, H. L. Contracted and Expanded *meso*-Alkynyl Porphyrinoids: from Triphyrin to Hexaphyrin. *J. Org. Chem.* **2003**, *68*, 1089−1096.
(22) Rexhausen, H.; Gossauer, A. The Synthesis of a New 22 π-Electron Macrocycle: Pentaphyrin. *J. Chem. Soc., Chem. Commun.* **1983**, 275.
(23) Lin, Y.; Lash, T. D. Porphyrin synthesis by the "3+1" methodology: a superior approach for the preparation of porphyrins with fused 9,10-phenantroline subunits. *Tetrahedron Lett.* **1995**, *36*, 9441−9444.
(24) Lash, T. D. Porphyrins with exocyclic rings. Part 9 [1] synthesis of porphyrins by the "3+1" approach. *J. Porphyrins Phthalocyanins* **1997**, *1*, 29−44.
(25) Sessler, J. L.; Johnson, M. R.; Linch, V. Synthesis and crystal structures of a novel tripyrrane-containing porphyrogen-like macrocycle. *J. Org. Chem.* **1987**, *52*, 4394−4397.
(26) Clarke, O. J.; Boyle, R. W. Selective synthesis of asymmetrically substituted 5,15- diphenylporphyrins. *Tetrahedron Lett.* **1998**, *39*, 7167−7168.
(27) Bruckner, C.; Posakony, J. F.; Johnson, C. K.; Boyle, R. W.; James, B. R.; Dolphin, D. Novel and Improved Syntheses of 5,15-Diphenylporphyrin and its Dipyrrolic Precursors. *J. Porphyrins Phthalocyanines* **1998**, *2*, 455−465.
(28) Brinas, R. P.; Bruckner C. Synthesis of 5,10-diphenylporphyrin. *Tetrahedron* **2002**, *58*, 4375−4381.
(29) Littler, B. J.; Miller, M. A.; Hung, C.; Wagner, R. W.; O'Shea, D. F.; Boyle, P. D.; Lindsey, J. S. Refined Synthesis of 5-Substituted Dipyrromethanes. *J. Org. Chem.* **1999**, *64*, 1391−1396.
(30) Kral, V.; Brucker, E. A.; Hemmi, G.; Sessler, J. L.; Kralova, J.; Bose, H., Jr. A non-ionic water-soluble pentaphyrin derivatives. Synthesis and cytotoxicity. *Bioorg. Med. Chem.* **1995**, *3*, 573−578.
(31) Fhurhop, J. H.; Demoulin, C.; Boettcher, C.; Koning, J.; Siggel, U. Chiral micellar porhyrin fibers with 2-aminoglycosamide headgroups. *J. Am. Chem. Soc.* **1992**, *114*, 4159.
(32) Haughland, R. P. Handbook of fluorescent probes and research chemicals. In Spence, M. T. Z., Ed.; *Nucleic Acids Detection*; Molecular Probes: Eugene, OR; pp 143−168.
(33) Moan, J.; Berg, K. Porphyrin photosensitization and phototherapy. *Photochem. Photobiol.* **1986**, *43*, 681−690.
(34) Guzburg, W. H.; Salmons, B. Novel clinical strategies for the treatment of pancreatic carcinoma. *Trends Mol. Med.* **2001**, *7*, 30−37.
(35) Sylvain, I.; Zerrouki, R.; Granet, R.; Huang, Y. M.; Lagorce, J.-F.; Guilloton, M.; Blais, J.-C.; Krausz, P. Synthesis and biological evaluation of thioglycosylated porphyrins for an application in photodynamic therapy. *Bioorg. Med. Chem.* **2002**, *10*, 57−69.
(36) Agarwal, M. L.; Clay, M. E.; Harvey, E. J.; Evans, H. H.; Antunez, A. R.; Oleinick, N. L. Photodynamic therapy induces rapid cell death by apoptosis in L5178Y mouse lymphoma cells. *Cancer Res.* **1991**, *51*, 5993−5996.
(37) Vaux, D. L.; Strasser, A. The molecular biology of apoptosis. *Proc. Natl. Acad. Sci. U.S.A.* **1996**, *93*, 2239−2244.
(38) Hickman, J. A.; Potten, C. S.; Meritt, A. J.; Fisher, T. C. Apoptosis and cancer chemiotherapy. *Philos. Trans R Soc. London B Biol. Sci.* **1994**, *345*, 319−325.
(39) Darzynkiewicz, Z.; Bruno, S.; Del Bino, S.; Gorzyca, W.; Hotz, M. A.; Bassotta, P.; Traganos, F. Features of apoptotic cells measured by flow cytometry. *Cytometry* **1992**, *13*, 795−808.
(40) Riedl, S.; Shi, T. Molecular mechanism of caspase regulation during apoptosis. *Nat. Rev. Mol. Cell Biol.* **2004**, *5*, 897−907.
(41) Agostinis, P.; Buytaert, E.; Breyssens, H.; Hendrickx, N. Regulatory pathways in photodynamic therapy induced apoptosis. *Photochem. Photobiol. Sci.* **2004**, *3*, 721−729.
(42) Oleinick, N. L.; Morris, R. L.; Belichenko, I. The role of apoptosis in response to photodynamic therapy: what, where, why, and how. *Photochem. Photobiol. Sci.* **2002**, *1*, 1−21.

JM050831L